Send Orders for Reprints to reprints@benthamscience.net

Anti-Cancer Agents in Medicinal Chemistry, 2022, *22*, 1-10

RESEARCH ARTICLE

Galbanic Acid Improves Accumulation and Toxicity of Arsenic Trioxide in MT-2 Cells

Maryam Mahdifar[1], Fatemeh B. Rassouli[2,*], Mehrdad Iranshahi[3], Sajad Goudarzi[4], Marzieh Golizadeh[5], Houshang Rafatpanah[6,*]

[1]*Inflammation and Inflammatory Diseases Research Center, Faculty of Medicine, Mashhad University of Medical Sciences, Mashhad, Iran;* [2]*Novel Diagnostics and Therapeutics Research Group, Institute of Biotechnology, Ferdowsi University of Mashhad, Mashhad, Iran;* [3]*Department of Pharmacognosy and Biotechnology, Biotechnology Research Center, Faculty of Pharmacy, Mashhad University of Medical Sciences, Mashhad, Iran;* [4]*Cancer Molecular Pathology Research Center, Department of Hematology and Blood Bank, Faculty of Medicine, Mashhad University of Medical Sciences, Mashhad, Iran;* [5]*Inflammation and Inflammatory Diseases Research Center, Faculty of Medicine, Mashhad University of Medical Sciences, Mashhad, Iran;* [6]*Inflammation and Inflammatory Diseases Research Center, Faculty of Medicine, Mashhad University of Medical Sciences, Mashhad, Iran*

Abstract: ***Background*:** Galbanic acid (GBA) is a sesquiterpene coumarin with valuable pharmacological effects. Adult T-cell lymphoma (ATL) is an aggressive lymphoid malignancy with a low survival rate. Although arsenic trioxide (ATO) is a standard therapeutic agent for ATL treatment, the efficacy of chemotherapy is limited due to the chemoresistance of cells.

***Objective*:** The present study was carried out to investigate whether GBA in combination with ATO would improve cytotoxicity against ATL cells.

***Methods*:** GBA was isolated from the roots of *Ferula szowitsiana* by column chromatography on silica gel. MT-2 cells were treated with 20 µM GBA + 4 µM ATO, and viability was evaluated by alamarBlue assay. The cell cycle was analyzed by PI staining, while the activity of P-glycoprotein (P-gp) was evaluated by mitoxantrone efflux assay. To understand the molecular mechanisms of GBA effects, the expression of *NF-κB (RelA), P53, CDK4, c-MYC, c-FLIPL,* and *c-FLIPS* was evaluated using real-time PCR.

***Results*:** Combinatorial use of GBA + ATO significantly reduced the viability of MT-2 cells and induced cell cycle arrest in the sub-G_1 phase. GBA improved mitoxantrone accumulation in cells, indicating that this agent has inhibitory effects on the functionality of the P-gp efflux pump. Moreover, real-time PCR analysis revealed that GBA + ATO negatively regulated the expression of *P53, CDK4, c-FLIPL,* and *c-FLIPS*.

***Conclusion*:** Due to the interesting effects of GBA on the accumulation and toxicity of ATO, combinatorial use of these agents could be considered a new therapeutic approach for ATL treatment.

Keywords: Galbanic acid, adult T cell leukemia, arsenic trioxide, drug accumulation, combination treatment, improved cytotoxicity.

ARTICLE HISTORY

Received: March 29, 2022
Revised: May 27, 2022
Accepted: June 03, 2022

DOI:
10.2174/1871520622666220722105802

1. INTRODUCTION

Adult T cell leukemia (ATL) is a highly aggressive peripheral T cell neoplasm associated with human T cell leukemia virus type 1 (HTLV-1) and is usually accompanied by visceral involvement [1]. It has been estimated that between 10 and 20 million people are infected with HTLV-1 worldwide, and approximately 3-5% of HTLV-1 infected subjects develop ATL [2]. HTLV-1 infected cells express viral Tax protein that induces *c-FLIP* and *c-MYC* and activates signaling pathways, such as Akt [3-5]. In addition, Tax activates NF-κB, which influences the survival and proliferation of ATL clones [6], and interacts with cyclin-dependent kinase inhibitor P16, which leads to the activation of CDK4 and consequently, promotes cell cycle *via* phosphorylation of RB [7].

ATL is clinically characterized by lymphadenopathy, generalized lymph node swelling, hepatosplenomegaly, skin lesions, hypercalcemia, increased number of abnormal lymphocytes, and increased susceptibility to opportunistic infections, including Candida species, cytomegalovirus, and pneumocystis jiroveci [8]. ATL is associated with poor prognosis and has a shorter *overall survival than* other peripheral T cell lymphomas. Several therapeutic approaches, such as multi-agent chemotherapy, anti-viral therapy and allogeneic hematopoietic stem cell transplantation, are currently available, although their clinical outcomes are unsatisfactory [1, 9]. The main reasons for inefficient ATL treatment are inherent chemoresistance and immunosuppression, which increases the susceptibility of patients to infection [10]. Hence, introducing novel multimodal approaches to deal with challenges in ATL management has great research value.

Arsenic trioxide (ATO) has been established as a potential therapy for patients with acute promyelocytic leukemia, chronic myeloid leukemia, and a number of solid tumors [11]. The inhibitory effects of ATO on hematological malignancies are associated with induction of oxidative damage, cell cycle arrest, and epigenetic

*Address correspondence to these authors at the Novel Diagnostics and Therapeutics Research Group, Institute of Biotechnology, Ferdowsi University of Mashhad, Mashhad, Iran; E-mail:. behnam3260@um.ac.ir
Inflammation and Inflammatory Diseases Research Center, Faculty of Medicine, Mashhad University of Medical Sciences, Mashhad, Iran; E-mail: rafatpanahh@mums.ac.ir

regulation. However, its application has been limited due to unfavorable side effects. Therefore, the therapeutic potential of ATO (at low concentrations) in combinatorial approaches is under investigation [12]. Treating HTLV-1 infected cells with ATO revealed that this agent induced its therapeutic effects by inhibiting cell proliferation or inducing apoptosis [13, 14]. In addition, combination therapy with ATO triggers the degradation of Tax oncoprotein and consequently inactivates NF-κB signaling pathway, which culminates in cell death [15, 16].

Galbanic acid (GBA) is a bioactive sesquiterpene coumarin isolated from *Ferula* species [17]. *Ferula assafoetida* and *Ferula Szowitsiana*, as rich sources of GBA, are herbaceous plants of the Umbelliferae family distributed throughout central Asia, eastern Iran, and Afghanistan [18, 19]. GBA possesses multiple biological activities, including anti-oxidative, anti-viral, hepatoprotective and anti-cancer effects [20-25]. GBA exerts its anti-cancer activity in association with apoptosis induction, anti-proliferative actions, and inhibition of P-glycoprotein (P-gp), an ATP-dependent efflux pump involved in resistance to chemical agents [23, 26]. Although anti-cancer and synergic effects of GBA have been investigated in several malignancies, the pharmaceutical effects of this valuable agent, in single-use or in combination with chemotherapeutic drugs, have not been indicated in ATL. Accordingly, the present study was designed to determine whether GBA, alone or in combination with ATO, could improve the therapeutic efficacy against ATL. In this regard, cell viability, cell cycle, efflux activity of P-gp and expression of *NF-κB (RelA)*, *P53, CDK4, c-MYC, c-FLIPL*, and *c-FLIPS* were investigated upon GBA and ATO administration.

2. MATERIALS AND METHODS

2.1. Isolation of GBA

GBA ($C_{24}H_{30}O_5$, 2-cyclohexene-1-butanoic acid) was extracted from the roots of *Ferula szowitsiana* by a previously described method [19]. Briefly, the roots of *F. szowitsiana* were air-dried at room temperature, triturated and extracted with acetone by presoaking with changing the solution thrice for 48 h at room temperature. The combined solvent extracts were vaporized to yield a brownish, viscous residual (8% yield). The residual was then dissociated by thin layer chromatography on silica gel using petroleum ether/ethyl acetate (2:1) as solvent. Visualizing the fractions was performed by UV at 254 nm. Fractions were deterged with acetone (Merck, Germany), and the active constituent was abundantly purified using the following method; Part of the extract (15 g) was exposed to column chromatography on silica gel (5×50cm) using petroleum ether with increasing volumes of acetone [petroleum ether (100), petroleum ether–acetone (95:5), (90:10), (85:15), (80:20), (75:25), (70:30), (60:40), (50:50) and acetone (100)].

To prepare different concentrations of GBA, at first, 2 mg of GBA was dissolved in 100 µl dimethyl sulfoxide (DMSO, Merck, Germany). Then, serial two-fold dilutions of GBA were prepared using DMSO, and final concentrations were obtained by culture medium. To avoid misinterpretation of the results due to toxic effects of DMSO, equal amounts of the solvent in all GBA concentrations (0.5% v/v) were considered as the control.

2.2. Cell Culture

MT-2 cell line (HTLV-1 transformed human T cells) was obtained from Pasteur Institute, Tehran, Iran. Cells were cultured in RPMI 1640 (KBC, Iran) medium supplemented with 10% fetal bovine serum (Gibco, USA), 1% penicillin/streptomycin (Capricorn, Germany) and 0.5% L- glutamine (Serena, Germany), and incubated at 37°C with 5% CO_2 and a humidity of 96%.

2.3. Cytotoxicity Assay

MT-2 cells were seeded at the density of 50×10^3 cells/well in 96-well plates and treated with various concentrations of GBA (5, 10, 20, 40, and 80 µM) for 24, 48, and 72 h. Meanwhile, cells were treated with 2, 4, 8, and 16 µM ATO (Sigma, Germany) for 3 consecutive days. At the end of each time point, the viability of cells was evaluated by alamarBlue assay. In this regard, 20 µl alamarBlue solution (0.15 g/ml, Sigma, Germany) was added to each well, and cells were incubated until a pink fluorescent resorufin was constituted. Then, optical density (OD) was measured at 600 nm using a microplate reader (Epoch, BioTek, USA), and viability (%) was calculated by the following formula: (100-(AT-AU)/(AB-AU)) × 100, in which AT, AU, and AB represent the absorbance of treated cells, untreated cells, and blank control, respectively. For combinatorial treatment, MT-2 cells were treated with GBA (5, 10 and 20 µM) + ATO (2 and 4 µM), concentrations less than their IC_{50} values, and assessed for viability after 24, 48, and 72 h.

2.4. Cell Cycle Analysis

To investigate changes induced in the cell cycle upon treatment with GBA, ATO, and their combination, MT-2 cells were seeded at the density of 40×10^4 cell/well in 6-well plates and treated with 20 µM GBA, 4 µM ATO, 20 µM GBA + 4 µM ATO and their relevant DMSO controls for 48 h. Then, cells were washed and resuspended in 480 µl of propidium iodide (PI) staining solution, consisting of 100 µg/mL PI (Sigma, Germany), 0.1% Triton X-100 (Sigma, Germany), and 0.1% sodium citrate (Merck, Germany) in PBS, and incubated at 37°C for 30 min in the dark. Finally, flow cytometry analysis was performed by FACS Calibur (BD Biosciences, USA) using an FL2 filter, and data were analyzed with winMDI data analysis software version 2.8.

2.5. Efflux Assay

To study the effect of GBA on P-gp activity, MT-2 cells were seeded at the density of 40×10^4 cells/well in 6-well plates and treated with 20 µM GBA for 48 h, while untreated cells and cells treated with 0.5% DMSO were considered as controls. After centrifugation, cell pellets were resuspended in mitoxantrone (10 µM, Sigma, Germany) and incubated at 37°C for 30 min in the dark (accumulation phase). After washing with ice-cold PBS twice, cells were resuspended in a culture medium and incubated at 37°C for 60 min in the dark (efflux phase). Finally, the activity of P-gp was analyzed by FACS Calibur (BD Biosciences, USA) using an FL3 filter and data were analyzed with winMDI data analysis software version 2.8.

2.6. Real-time PCR

To understand the molecular mechanisms of our combinatorial approach, the expression of candidate genes was evaluated by real-time PCR. Briefly, total RNA was extracted from MT-2 cells treated with 20 µM GBA, 4 µM ATO and their combination, as well as their relevant controls, using Tripure isolation reagent (Roche, Germany) according to the manufacturer's instruction. Then, cDNA was synthesized using reverse transcriptase and random primers according to the manufacturer's protocol (Thermo Fisher Scientific, USA), followed by PCR with β2 microglobulin (β2M) primers. For real-time PCR, primers and probes were designed by Allele ID, version 5, after obtaining the desired sequences for genes *NF-κB (RelA), P53, CDK4, c-MYC, c-FLIPL,* and *c-FLIPS* from the National Center for Biotechnology Information (NCBI) GenBank. Real-time PCR was performed in Rotor gene 6000 cycler (Qiagen, Germany), using TaqMan (for *NF-κB (RelA), P53,* and *CDK4*) and SYBR green (for *c-MYC, c-FLIPL,* and *c-FLIPS*), while *β2M* was considered as the cellular reference gene in both methods. Table **1** represents specific primers and probes used in the present study.

2.7. Statistical Analysis

Statistical analysis was performed using Statistical Package for Social Sciences (SPSS) software (version 16.0, SPSS, Inc, Chicago,

Table 1. Primer and probe sequences and amplicon lengths.

Name	Primer Name	Sequence (5'→3')	Product Length (bp)
c-MYC	Forward	ACTCTGAGGAGGAACAAGAA	159
-	Reverse	TGGAGACGTGGCACCTCTT	-
c-FLIPL	Forward	ATTGGCAATGAGACAGAGCTTC	126
-	Reverse	CTCGGGCATACAGGCAAA	-
c-FLIPS	Forward	CCAGAAGTACAAGCAGTCTGTTC	122
-	Reverse	GGGCATAGGGTGTTATCATCC	-
β2M	Forward	AATTGAAAAAGTGGAGCATTCAGA	127
-	Reverse	GGCTGTGACAAAGTCACATGGTT	-
NF-κB (RelA)	Forward	ACCCCTTCCAAGTTCCTATAGAAGAG	145
-	Reverse	CGATTGTCAAAGATGGGATGAGAAAG	-
-	Probe	ACTACGACCTGAATGCTGTGCGGCTCTG	-
P53	Forward	CAGCATCTTATCCGAGTGGAAGG	132
-	Reverse	GTTGTAGTGGATGGTGGTACAGTC	-
-	Probe	CTCAGGCGGCTCATAGGGCACCAC	-
CDK4	Forward	AAATTGGTGTCGGTGCCTATGG	135
-	Reverse	CACGAACTGTGCTGATGGGAAG	-
-	Probe	ACAAGGCCCGTGATCCCCACAGTGG	-
β2M	Forward	TTGTCTTTCAGCAAGGACTGG	127
-	Reverse	CCACTTAACTATCTTGGGCTGTG	-
-	Probe	TCACATGGTTCACACGGCAGGCAT	-

IL, USA). Variables were compared between groups by one-way ANOVA and Bonferroni post-hoc tests. For gene expression analysis, Spearman's correlation test was used. p values <0.05, <0.01, <0.001, and < 0.0001 were considered to be statistically significant. All data were expressed as mean ± standard deviation (SD).

3. RESULTS

3.1. High Concentrations of GBA Exerted Cytotoxicity on MT-2 Cells

Viability assessment of MT-2 cells indicated that GBA induced its toxic effects in a time- and dose-dependent manner. As presented in Fig. (**1**), only the highest concentration of GBA (80 µM) significantly ($p<0.001$) decreased viability after 24 h. Nevertheless, GBA toxicity increased upon to 48 h, as 40 and 80 µM GBA significantly ($p<0.0001$) reduced cell viability, and this effect was limited to 80 µM GBA in the last time point (72 h). The IC_{50} values of GBA and ATO were calculated as 80 and 16 µM after 72 h, respectively.

3.2. GBA Improved the Toxicity of ATO

In order to study the combinatorial effects of GBA and ATO, the viability of cells was evaluated after treatment with GBA (5, 10, and 20 µM) + ATO (2 and 4 µM), alongside their relevant controls, including 0.5% DMSO + ATO (2 and 4 µM). As presented in Fig. (**2A**), the viability of cells was significantly ($p<0.05$ and $p<0.0001$) reduced by GBA (5, 10, and 20 µM) + ATO (4 µM) after 24 h, which indicated improved effects of 4 µM ATO by all concentrations of GBA. When treatment was extended up to 48 h, 10 and 20 µM GBA significantly ($p<0.05$ and $p<0.0001$) improved the toxicity of 2 and 4 µM ATO (Fig. **2B**). In addition, 5 µM GBA significantly ($p<0.01$) increased the cytotoxicity of 4 µM ATO after 48 h. However, after 72 h of treatment of cells, a significant ($p<0.001$) increase in toxicity was only observed when 20 µM GBA + 4 µM ATO were used (Fig. **2C**).

3.3. Combination of GBA and ATO Induced Cell cycle Arrest in the Sub-G_1 Phase

Flow cytometry analysis of the cell cycle was performed to determine whether combinatorial effects of GBA and ATO were associated with cell cycle changes. As shown in Fig. (**3**), combination of 20 µM GBA + 4 µM ATO induced significant cell cycle arrest in the sub-G_1 phase (55.56%), when compared with 20 µM GBA (2.3%), 4 µM ATO (4.03%) and 0.5% DMAO + 4 µM ATO (3.28%).

3.4. GBA Decreased the Efflux Activity of P-gp

To determine whether GBA affects the efflux activity of P-gp, MT-2 cells were treated with 20 µM GBA for 48 h. Then P-gp-mediated mitoxantrone efflux was assessed by flow cytometry. As shown in Fig. (**4**), treatment of cells with GBA increased mitoxantrone accumulation in MT-2 cells (indicated by the right shift of the histogram) when compared with untreated and 0.5% DMSO treated cells.

3.5. GBA, Alone and in Combination with ATO, Negatively Regulated the Expression of Candidate Genes

To unravel the mechanism of GBA action in our study, the expression of *NF-κB (RelA), P53, CDK4, c-MYC, c-FLIPL,* and *c-FLIPS* was evaluated by real-time PCR. As shown in Fig. (**5**), the expression of *NF-κB (RelA), P53, CDK4, c-MYC,* and *c-FLIPS* was reduced by 20 µM GBA when compared to 0.5% DMSO. Nevertheless, significant decrease was only calculated for *NF-κB (RelA)* (0.025 ± 0.003, $p< 0.0001$), *CDK4* (0.09 ± 0.006, $p< 0.0001$), and *c-MYC* (0.64 ± 0.3, $p< 0.001$). For combinatorial use of 20 µM GBA + 4 µM ATO, negative regulation of all genes was observed when compared with its relevant control (0.5% DMSO + 4 µM ATO), although it was only significant for *P53* (0.03 ± 0.002, $p< 0.0001$), *CDK4* (0.2 ± 0.01, $p< 0.0001$), *c-FLIPL* (0.22 ± 0.1, $p< 0.01$), and *c-FLIPS* (0.12 ± 0.02, $p< 0.001$). In addition, there was a

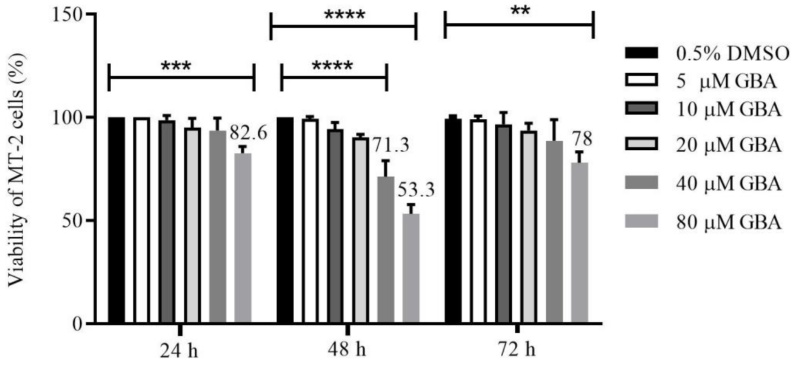

Fig. (1). Time-based dose-response analysis of MT-2 cells after GBA treatment. MT-2 cells were treated with increasing concentrations of GBA (5, 10, 20, 40, and 80 µM) for 24, 48, and 72 h, and viability was evaluated with an alamarBlue assay. $^{**}p < 0.01$, $^{***}p < 0.001$ and $^{****}p < 0.0001$ indicate significant difference with relevant control (0.5% DMSO). A viability assessment was carried out at least three times, and the results are presented as mean ± SD. (*A higher resolution / colour version of this figure is available in the electronic copy of the article*).

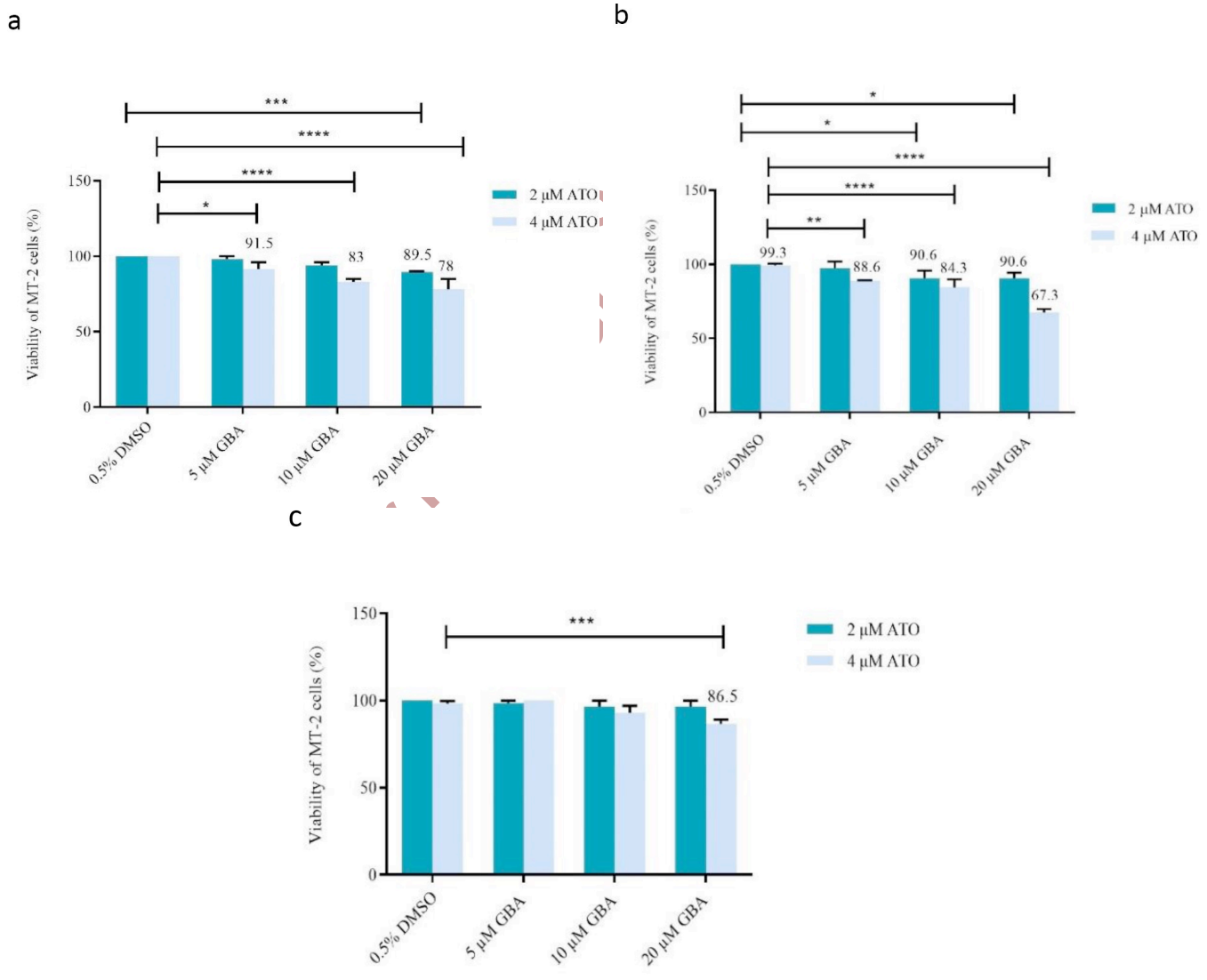

Fig. (2). Viability of MT-2 cells upon treatment with the combination of GBA + ATO during 3 consecutive days. Cells were treated with GBA (5, 10 and 20 µM) + ATO (2 and 4 µM), and viability was assessed after 24 (**a**), 48 (**b**) and 72 (**c**) h. $^{*}p < 0.05$, $^{**}p < 0.01$, $^{***}p < 0.001$ and $^{****}p < 0.0001$ indicate significant difference with relevant control (0.5% DMSO + ATO with similar doses). A viability assessment was carried out at least three times, and the results are presented as mean ± SD. (*A higher resolution / colour version of this figure is available in the electronic copy of the article*).

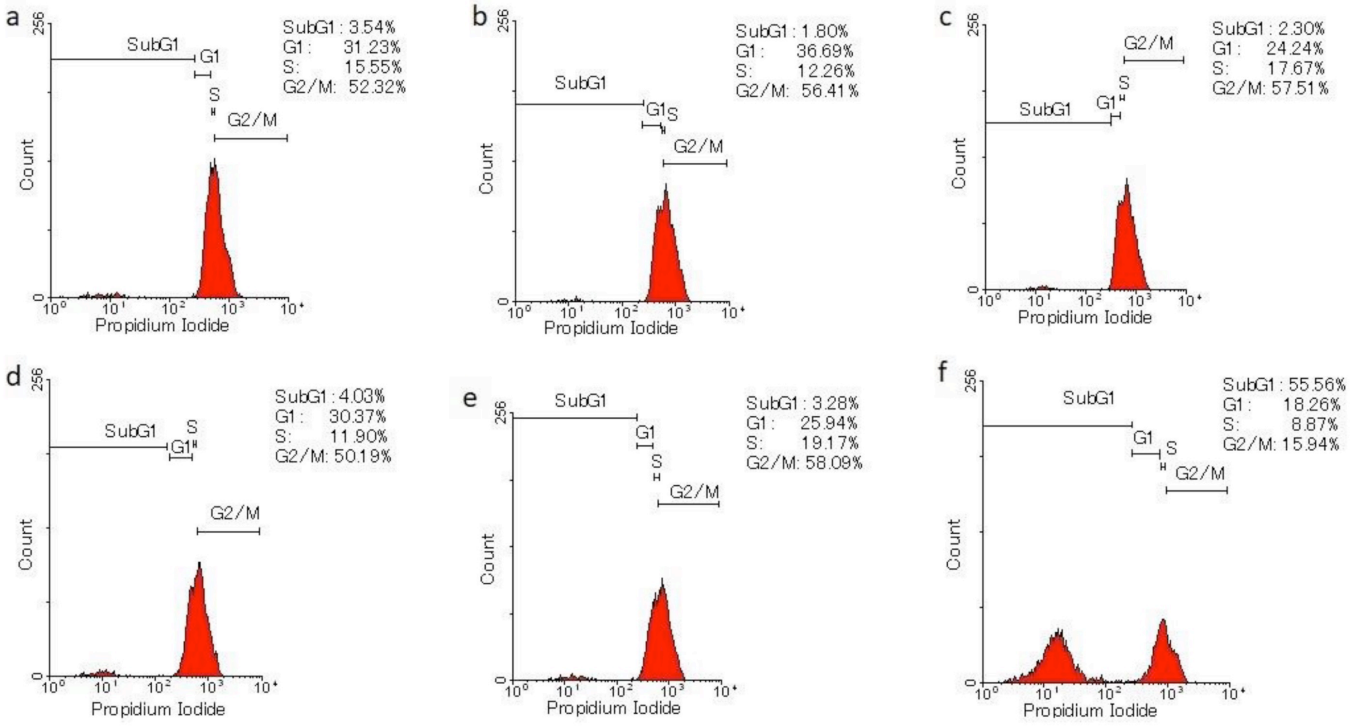

Fig. (3). Changes induced in the cell cycle by GBA, ATO and their combination. MT-2 cells were treated with 20 µM GBA, 4 µM ATO, and their combination for 48 h. PI staining revealed the distribution of cells in the sub-G_1, G_1, S and G_2/M phases of the cell cycle. Untreated cells (**a**) and cells treated with 0.5% DMSO (**b**), 20 µM GBA (**c**), 4 µM ATO (**d**), 0.5% DMSO + 4 µM ATO (**e**) and 20 µM GBA + 4 µM ATO (**f**). (*A higher resolution / colour version of this figure is available in the electronic copy of the article*).

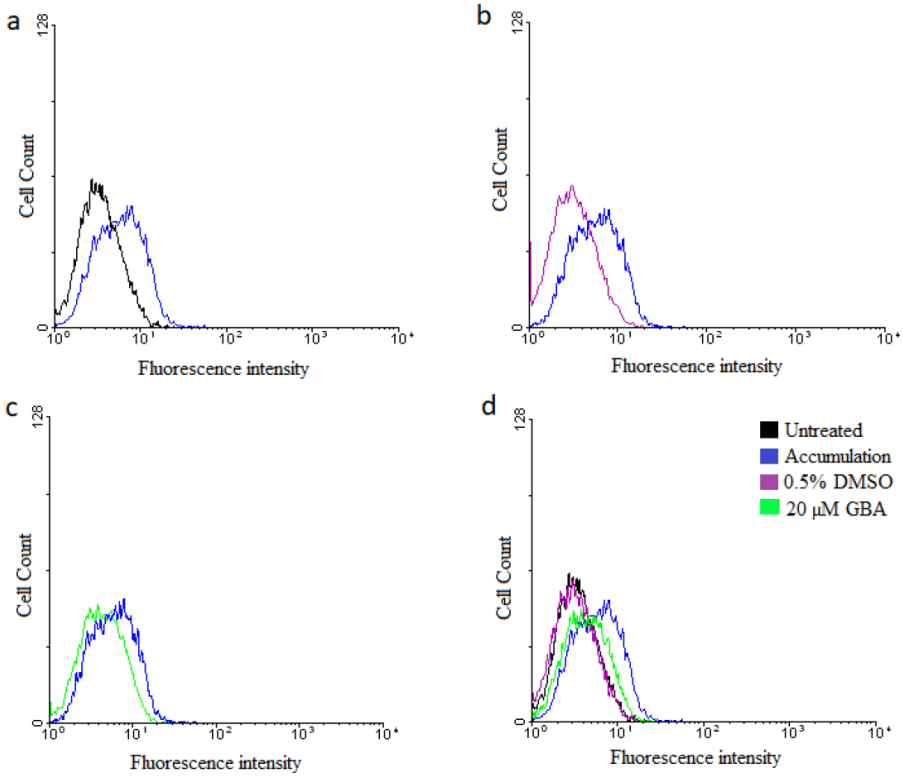

Fig. (4). Flow cytometry analysis of mitoxantrone uptake and efflux by MT-2 cells. P-gp function was assayed after exposure to mitoxantrone in untreated cells (**a**) and cells treated with 0.5% DMSO (**b**) and 20 µM GBA (**c**) for 48 h. As shown by the right shift in fluorescence, GBA decreased mitoxantrone efflux in MT-2 cells compared to controls (**d**). The fluorescence of 10000 cells was quantified from histogram plots. (*A higher resolution / colour version of this figure is available in the electronic copy of the article*).

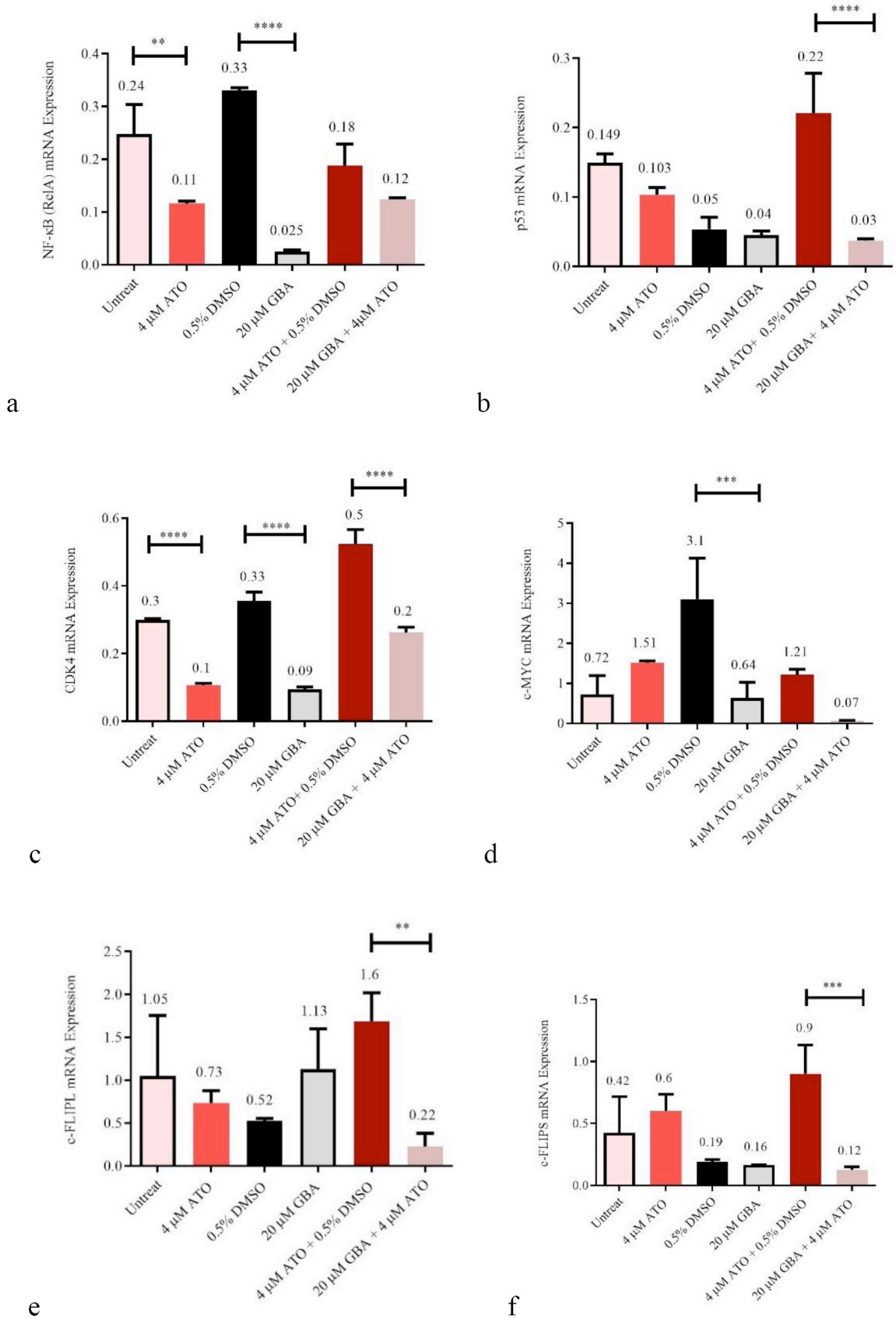

Fig. (5). Expression pattern of *NF-κB (RelA)* (**a**), *P53* (**b**), *CDK4* (**c**), *c-MYC* (**d**), *c-FLIPL* (**e**), and *c-FLIPS* (**f**) in MT-2 cells after single and combinatorial treatments with GBA and ATO. $^{**}p < 0.01$, $^{***}p < 0.001$ and $^{****}P < 0.0001$ indicate significant difference with relevant controls (untreated, 0.5% DMSO or 0.5% DMSO + ATO). Results are presented as mean ± SD. (*A higher resolution / colour version of this figure is available in the electronic copy of the article*).

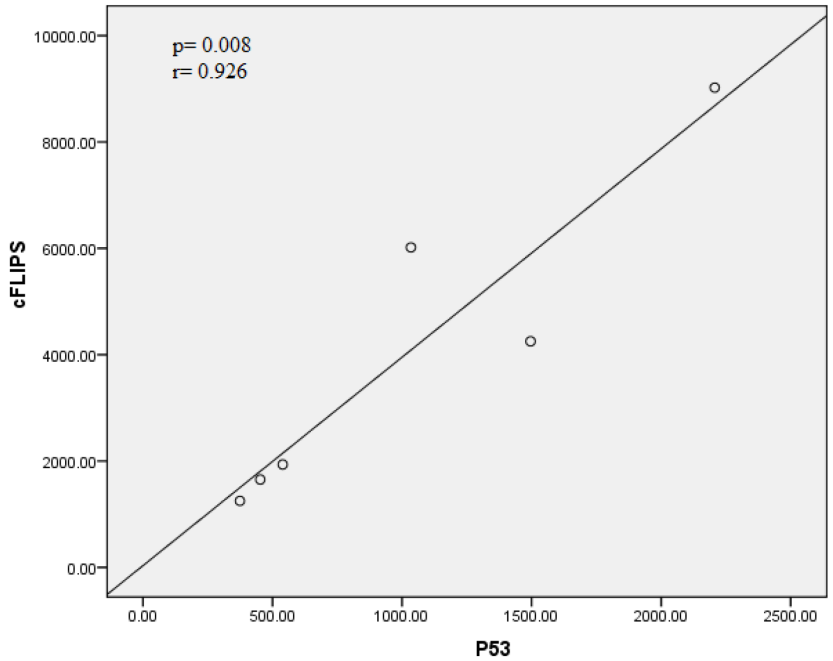

Fig. (6). Pearson's correlation analysis for the expression of *P53* and *c-FLIPS* in 6 groups; untreated MT-2 cells and cells treated with 20 µM GBA, 4 µM ATO, 20 µM GBA + 4 µM ATO, 0.5% DMSO and 0.5% DMSO + 4 µM ATO. (*A higher resolution / colour version of this figure is available in the electronic copy of the article*).

significant positive correlation between the expression of *c-FLIPS* and *P53* (p= 0.008 and r= 0.926) (Fig. **6**).

4. DISCUSSION

ATL is an aggressive malignancy of mature T cells. Since current multi-agent chemotherapy regimens may not provide long-term survival for ATL patients, the development of more efficient combined chemotherapy regimens is one of the main scopes in ATL research [1]. ATO is a potential chemotherapeutic agent that is used in combination with anti-viral agents and IFN-α for ATL treatment [27]. However, unfavorable side effects of ATO limit its clinical applications. In the present study, we aimed to determine whether GBA, as a valuable pharmaceutical agent, could improve the efficacy of ATO in ATL cells.

GBA is a natural sesquiterpene coumarin with considerable anti-viral and anti-cancer activities [19, 21-23, 26]. Results of the present study indicated that GBA induced toxic effects on MT-2 cells in a dose- and time-dependent manner. Previous studies have also reported dose-depended effects of GBA on human ovarian and lung carcinoma cells, as well as umbilical vein epithelial cells [23, 28, 29]. In addition, it has been shown that a combination of GBA and TNF-related apoptosis-inducing ligand (TRAIL) induced toxic effects on chemo-resistant lung cancer cells, while combinatorial use of GBA and nanomicellar curcumin showed toxicity on murine and human colon carcinoma cells [30, 31]. Our findings indicated, for the first time, that combinatorial use of GBA and ATO induced more toxic effects on ATL cells than a single administration of each agent. Improved toxicity of ATO by GBA was confirmed *via* accumulation of cells in the sub-G_1 phase of the cell cycle. In line with present results, it has been reported that GBA inhibited cell cycle progression through induction of G_1 or sub-G_1 arrest in prostate and lung cancer cells [32, 33]. Moreover, the combination of GBA and TRAIL increased the sub-G_1 apoptotic population in resistant lung carcinoma cells [31]. Similarly, the combination of ATO with other natural coumarin and sesquiterpene derivatives induced cytotoxicity and cell cycle arrest. In this regard, it has been demonstrated that combinatorial use of ATO with auraptene, umbelliprenin, and parthenolide led to the accumulation of ATL cells in the sub-G_1 phase of the cell cycle [34-36].

Pumping therapeutic agents out of the cell, mediated by multiple drug efflux transporters, is a serious impediment to effective chemotherapy. Since Tax-mediated overexpression and enhanced efflux activity of P-gp have been reported in ATL [37], agents that inhibit P-gp activity could be used in combination with existing medicines to increase clinical outcomes. It has been indicated that GBA inhibited P-gp activity in chemo-resistant breast and lung cancer cells [26, 31]. Current findings are in agreement with previous reports, as reduced efflux activity of P-gp pump was detected after GBA treatment of ATL cells.

To ascertain the possible mechanisms involved in GBA effects, we evaluated the expression of *NF-κB (RelA), P53, CDK4, c-MYC, c-FLIPL,* and *c-FLIPS* genes mainly attributed to cell proliferation, cell cycle progression, and apoptosis. HTLV-1 infection is correlated with immortalization, transformation and leukemogenesis of cells, and finally, ATL pathogenesis [4, 5, 38-44]. As presented in Fig. (**7**), HTLV-1 Tax oncoprotein alters the expression of specific genes; it induces *c-MYC*, *NF-κB,* and *c-FLIP*, while downregulating *P16* (a negative regulator of CDK4) and *P53* [3-7]. Obtained findings indicated that single administration of GBA negatively regulated *NF-κB (RelA), CDK4,* and *c-MYC*, while its combinatorial use with ATO reduced the expression of *CDK4*, *P53, c-FLIPL,* and *c-FLIPS* in ATL cells. CDK4 mediates G_1/S cell cycle progression [45], and Tax protein interacts with inhibitors of CDK, such as P16, leading to cell cycle progression and uncontrolled proliferation [7, 39, 42]. Hence, negative regulation of *CDK4* by GBA might explain the accumulation of ATL cells in the sub-G_1 phase, as downregulation of CDK4 inhibits the transition from G_1 to S phase of the cell cycle. Elevated expression of *c-FLIP* supports cancer cells to elude immunosurveillance and promotes proliferation [46, 47]. Tax expressing HTLV-1 infected T cells express a high level of *c-FLIPL* and *c-FLIPS* that contributes to inhibition of apoptosis, blocks the receptor-mediated cell death, evades the host immune response, and supports the development of HTLV-1-associated diseases [5, 48]. Accordingly, downregulation of *c-FLIPL* and *c-*

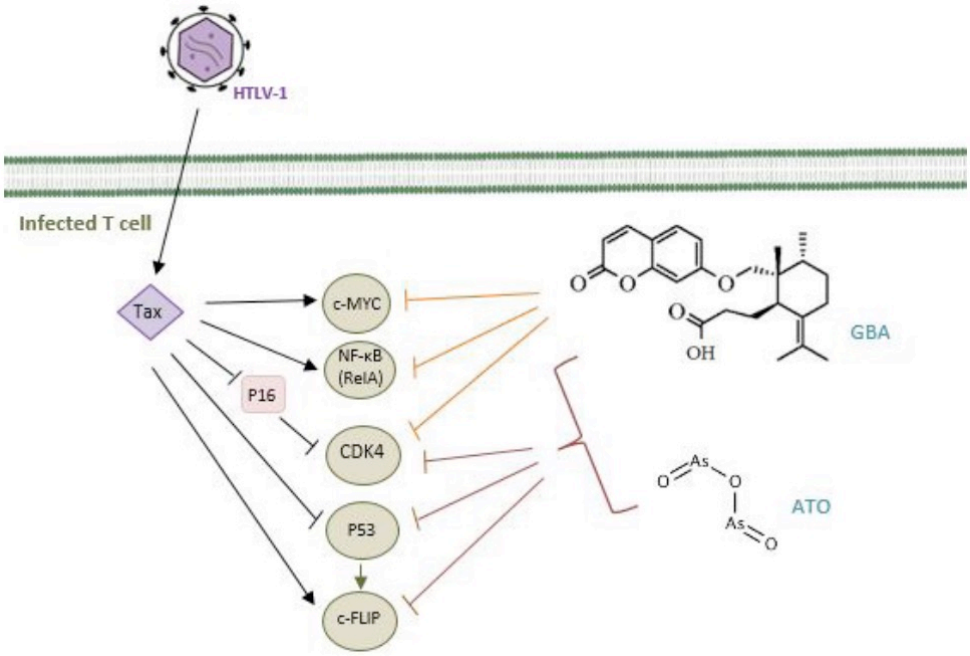

Fig. (7). Schematic representation of changes induced by HTLV-1 Tax protein and GBA in the expression of candidate genes. Tax induces *c-MYC*, *NF-κB* and *c-FLIP*, while downregulating *P16* and *P53* [3-7]. Results of the current study indicated that single use of GBA negatively regulated *NF-κB (RelA), CDK4* and *c-MYC*, while GBA + ATO reduced the expression of *CDK4*, *P53, c-FLIPL* and *c-FLIPS* in ATL cells. (*A higher resolution / colour version of this figure is available in the electronic copy of the article*).

FLIPS upon GBA + ATO treatment could augment death receptor-mediated apoptosis in MT-2 cells and thus, makes cells more susceptible to apoptosis. P53 plays a crucial role in cancer prevention by controlling the cell cycle progression and inducing apoptosis [49, 50]. In the current study, a significant positive correlation was found between the expression of *c-FLIPS* and *P53*, which could be explained by the positive involvement of P53 in *c-FLIPS* expression [51]. Since c-FLIP contributes to apoptosis resistance, downregulation of *P53* in MT-2 cells after GBA + ATO treatment might inhibit the P53-mediated upregulation of *c-FLIPS* and, therefore, reduces c-FLIPS inhibitory effects on apoptosis.

CONCLUSION

Findings of the present study demonstrated, for the first time, that GBA improves the accumulation and toxicity of ATO in MT-2 cells. Hence, combinatorial use of GBA and ATO could be considered an effective strategy for ATL treatment. However, complementary *in vitro* studies on other ATL cell lines would help to better evaluate GBA combinatorial effects and to elucidate its exact mechanism of action. Moreover, future *in vivo* studies and clinical trials are required to establish GBA as a safe and effective agent for ATL treatment.

ETHICS APPROVAL AND CONSENT TO PARTICIPATE

This study was approved by the Research Council of Mashhad University of Medical Sciences (IR.MUMS.MEDICAL.REC. 961916).

HUMAN AND ANIMAL RIGHTS

No animals/humans were used for studies that are the basis of this research.

CONSENT FOR PUBLICATION

Not applicable.

AVAILABILITY OF DATA AND MATERIALS

Not applicable.

FUNDING

This study was financially supported by the Research Council of Mashhad University of Medical Sciences (Grant Number: 961916).

CONFLICT OF INTEREST

The authors declare no conflict of interest, financial or otherwise.

ACKNOWLEDGEMENTS

Declared none.

REFERENCES

[1] Hermine, O.; Ramos, J.C.; Tobinai, K. A review of new findings in adult T-celllLeukemia-lymphoma: A focus on current and emerging treatment strategies. *Adv. Ther.*, **2018**, *35*(2), 135-152. http://dx.doi.org/10.1007/s12325-018-0658-4 PMID: 29411267

[2] Nagasaka, M.; Yamagishi, M.; Yagishita, N.; Araya, N.; Kobayashi, S.; Makiyama, J.; Kubokawa, M.; Yamauchi, J.; Hasegawa, D.; Coler-Reilly, A.L.G.; Tsutsumi, S.; Uemura, Y.; Arai, A.; Takata, A.; Inoue, E.; Hasegawa, Y.; Watanabe, T.; Suzuki, Y.; Uchimaru, K.; Sato, T.; Yamano, Y. Mortality and risk of progression to adult T cell leukemia/lymphoma in HTLV-1-associated myelopathy/tropical spastic paraparesis. *Proc. Natl. Acad. Sci. USA,* **2020**, *117*(21), 11685-11691. http://dx.doi.org/10.1073/pnas.1920346117 PMID: 32393644

[3] Cherian, M.A.; Baydoun, H.H.; Al-Saleem, J.; Shkriabai, N.; Kvaratskhelia, M.; Green, P.; Ratner, L. Akt pathway activation by human T-cell leukemia virus type 1 Tax oncoprotein. *J. Biol. Chem.,* **2015**, *290*(43), 26270-26281. http://dx.doi.org/10.1074/jbc.M115.684746 PMID: 26324707

[4] Duyao, M.P.; Kessler, D.J.; Spicer, D.B.; Bartholomew, C.; Cleveland, J.L.; Siekevitz, M.; Sonenshein, G.E. Transactivation of the c-myc promoter by human T cell leukemia virus type 1 tax is mediated by NF kappa B. *J. Biol. Chem.,* **1992**, *267*(23), 16288-16291. http://dx.doi.org/10.1016/S0021-9258(18)41998-9 PMID: 1644814

[5] Krueger, A.; Fas, S.C.; Giaisi, M.; Bleumink, M.; Merling, A.; Stumpf, C.; Baumann, S.; Holtkotte, D.; Bosch, V.; Krammer, P.H.; Li-Weber, M. HTLV-1 Tax protects against CD95-mediated apoptosis by induction of the cellular FLICE-inhibitory protein (c-FLIP). *Blood,* **2006**, *107*(10), 3933-3939. http://dx.doi.org/10.1182/blood-2005-06-2567 PMID: 16403915

[6] Harhaj, E.W.; Giam, C.Z. NF-κB signaling mechanisms in HTLV-1-induced adult T-cell leukemia/lymphoma. *FEBS J.,* **2018**, *285*(18), 3324-3336. http://dx.doi.org/10.1111/febs.14492 PMID: 29722927

[7] Suzuki, T.; Kitao, S.; Matsushime, H.; Yoshida, M. HTLV-1 Tax protein interacts with cyclin-dependent kinase inhibitor p16INK4A and counteracts its inhibitory activity towards CDK4. *EMBO J.,* **1996**, *15*(7), 1607-1614. http://dx.doi.org/10.1002/j.1460-2075.1996.tb00505.x PMID: 8612584

[8] Abeloff, M.D. *Abeloff's Clinical Oncology E-Book*; Elsevier Health Sciences, **2008**.

[9] Ishitsuka, K.; Tamura, K. Human T-cell leukaemia virus type I and adult T-cell leukaemia-lymphoma. *Lancet Oncol.,* **2014**, *15*(11), e517-e526. http://dx.doi.org/10.1016/S1470-2045(14)70202-5 PMID: 25281470

[10] Kchour, G.; Rezaee, R.; Farid, R.; Ghantous, A.; Rafatpanah, H.; Tarhini, M.; Kooshyar, M.M.; El Hajj, H.; Berry, F.; Mortada, M.; Nasser, R.; Shirdel, A.; Dassouki, Z.; Ezzedine, M.; Rahimi, H.; Ghavamzadeh, A.; de Thé, H.; Hermine, O.; Mahmoudi, M.; Bazarbachi, A. The combination of arsenic, interferon-alpha, and zidovudine restores an "immunocompetent-like" cytokine expression profile in patients with adult T-cell leukemia lymphoma. *Retrovirology,* **2013**, *10*(1), 91. http://dx.doi.org/10.1186/1742-4690-10-91 PMID: 23962110

[11] Lengfelder, E.; Hofmann, W.K.; Nowak, D. Impact of arsenic trioxide in the treatment of acute promyelocytic leukemia. *Leukemia,* **2012**, *26*(3), 433-442. http://dx.doi.org/10.1038/leu.2011.245 PMID: 21904379

[12] Wang, Q.Q.; Jiang, Y.; Naranmandura, H. Therapeutic strategy of arsenic trioxide in the fight against cancers and other diseases. *Metallomics,* **2020**, *12*(3), 326-336. http://dx.doi.org/10.1039/c9mt00308h PMID: 32163072

[13] Ishitsuka, K.; Ikeda, R.; Utsunomiya, A.; Uozumi, K.; Hanada, S.; Suzuki, S.; Takeuchi, S.; Takatsuka, Y.; Takeshita, T.; Ohno, N.; Arima, T. Arsenic trioxide induces apoptosis in HTLV-I infected T-cell lines and fresh adult T-cell leukemia cells through CD95 or tumor necrosis factor alpha receptor independent caspase activation. *Leuk. Lymphoma,* **2002**, *43*(5), 1107-1114. http://dx.doi.org/10.1080/10428190290021461 PMID: 12148893

[14] Mahieux, R.; Pise-Masison, C.; Gessain, A.; Brady, J.N.; Olivier, R.; Perret, E.; Misteli, T.; Nicot, C. Arsenic trioxide induces apoptosis in human T-cell leukemia virus type 1- and type 2-infected cells by a caspase-3-dependent mechanism involving Bcl-2 cleavage. *Blood,* **2001**, *98*(13), 3762-3769. http://dx.doi.org/10.1182/blood.V98.13.3762 PMID: 11739184

[15] Bazarbachi, A.; El-Sabban, M.E.; Nasr, R.; Quignon, F.; Awaraji, C.; Kersual, J.; Dianoux, L.; Zermati, Y.; Haidar, J.H.; Hermine, O.; de Thé, H. Arsenic trioxide and interferon-alpha synergize to induce cell cycle arrest and apoptosis in human T-cell lymphotropic virus type I-transformed cells. *Blood,* **1999**, *93*(1), 278-283. http://dx.doi.org/10.1182/blood.V93.1.278 PMID: 9864171

[16] El-Sabban, M.E.; Nasr, R.; Dbaibo, G.; Hermine, O.; Abboushi, N.; Quignon, F.; Ameisen, J.C.; Bex, F.; de Thé, H.; Bazarbachi, A. Arsenic-interferon-alpha-triggered apoptosis in HTLV-I transformed cells is associated with tax down-regulation and reversal of NF-kappa B activation. *Blood,* **2000**, *96*(8), 2849-2855. PMID: 11023521

[17] Iranshahi, M.; Rezaee, R.; Najaf Najafi, M.; Haghbin, A.; Kasaian, J. Cytotoxic activity of the genus *Ferula* (Apiaceae) and its bioactive constituents. *Avicenna J. Phytomed.,* **2018**, *8*(4), 296-312. PMID: 30377589

[18] Abd El-Razek, M.H.; Ohta, S.; Ahmed, A.A.; Hirata, T. Sesquiterpene coumarins from the roots of Ferula assa-foetida. *Phytochemistry,* **2001**, *58*(8), 1289-1295. http://dx.doi.org/10.1016/S0031-9422(01)00324-7 PMID: 11738424

[19] Iranshahi, M.; Arfa, P.; Ramezani, M.; Jaafari, M.R.; Sadeghian, H.; Bassarello, C.; Piacente, S.; Pizza, C. Sesquiterpene coumarins from Ferula szowitsiana and *in vitro* antileishmanial activity of 7-prenyloxycoumarins against promastigotes. *Phytochemistry,* **2007**, *68*(4), 554-561. http://dx.doi.org/10.1016/j.phytochem.2006.11.002 PMID: 17196626

[20] Iranshahi, M.; Kalategi, F.; Rezaee, R.; Shahverdi, A.R.; Ito, C.; Furukawa, H.; Tokuda, H.; Itoigawa, M. Cancer chemopreventive activity of terpenoid coumarins from Ferula species. *Planta Med.,* **2008**, *74*(2), 147-150. http://dx.doi.org/10.1055/s-2008-1034293 PMID: 18240102

[21] Iranshahy, M.; Iranshahi, M. Traditional uses, phytochemistry and pharmacology of asafoetida (Ferula assa-foetida oleo-gum-resin)-a review. *J. Ethnopharmacol.,* **2011**, *134*(1), 1-10. http://dx.doi.org/10.1016/j.jep.2010.11.067 PMID: 21130854

[22] Kasaian, J.; Iranshahy, M.; Iranshahi, M. Synthesis, biosynthesis and biological activities of galbanic acid–A review. *Pharm. Biol.,* **2014**, *52*(4), 524-531. http://dx.doi.org/10.3109/13880209.2013.846916 PMID: 25471377

[23] Kim, K.H.; Lee, H.J.; Jeong, S.J.; Lee, H.J.; Lee, E.O.; Kim, H.S.; Zhang, Y.; Ryu, S.Y.; Lee, M.H.; Lü, J.; Kim, S.H. Galbanic acid isolated from Ferula assafoetida exerts *in vivo* anti-tumor activity in association with anti-angiogenesis and anti-proliferation. *Pharm. Res.,* **2011**, *28*(3), 597-609. http://dx.doi.org/10.1007/s11095-010-0311-7 PMID: 21063754

[24] Shahcheraghi, S.H.; Lotfi, M.; Soukhtanloo, M.; Ghayour Mobarhan, M.; Jaliani, H.Z.; Sadeghnia, H.R.; Ghorbani, A. Effects of galbanic acid on proliferation, migration, andaApoptosis of glioblastoma cells through the PI3K/Akt/MTOR signaling pathway. *Curr. Mol. Pharmacol.,* **2021**, *14*(1), 79-87. http://dx.doi.org/10.2174/1874467213666200512075507 PMID: 32394847

[25] Hashemi, R. *In vitro* study of radiosensitivity effects of galbanic acid on ovarian tumor cells (OVCAR-3 Cell Line). *Nat. Prod. Commun.,* **2021**, *16*(10), 1934578X211046068.

[26] Hanafi-Bojd, M.Y.; Iranshahi, M.; Mosaffa, F.; Tehrani, S.O.; Kalalinia, F.; Behravan, J. Farnesiferol A from Ferula persica and galbanic acid from Ferula szowitsiana inhibit P-glycoprotein-mediated rhodamine efflux in breast cancer cell lines. *Planta Med.,* **2011**, *77*(14), 1590-1593. http://dx.doi.org/10.1055/s-0030-1270987 PMID: 21484672

[27] Kchour, G.; Tarhini, M.; Kooshyar, M.M.; El Hajj, H.; Wattel, E.; Mahmoudi, M.; Hatoum, H.; Rahimi, H.; Maleki, M.; Rafatpanah, H.; Rezaee, S.A.; Yazdi, M.T.; Shirdel, A.; de Thé, H.; Hermine, O.; Farid, R.; Bazarbachi, A. Phase 2 study of the efficacy and safety of the combination of arsenic trioxide, interferon alpha, and zidovudine in newly diagnosed chronic adult T-cell leukemia/lymphoma (ATL). *Blood,* **2009**, *113*(26), 6528-6532. http://dx.doi.org/10.1182/blood-2009-03-211821 PMID: 19411628

[28] Eskandani, M.; Abdolalizadeh, J.; Hamishehkar, H.; Nazemiyeh, H.; Barar, J. Galbanic acid inhibits HIF-1α expression *via* EGFR/HIF-1α pathway in cancer cells. *Fitoterapia,* **2015**, *101*, 1-11. http://dx.doi.org/10.1016/j.fitote.2014.12.003 PMID: 25510323

[29] Eskandani, M.; Barar, J.; Dolatabadi, J.E.; Hamishehkar, H.; Nazemiyeh, H. Formulation, characterization, and geno/cytotoxicity studies of galbanic acid-loaded solid lipid nanoparticles. *Pharm. Biol.,* **2015**, *53*(10), 1525-1538. http://dx.doi.org/10.3109/13880209.2014.991836 PMID: 25853953

[30] Jafari, A.; Teymouri, M.; Ebrahimi Nik, M.; Abbasi, A.; Iranshahi, M.; Hanafi-Bojd, M.Y.; Jafari, M.R. Interactive anticancer effect of nanomicellar curcumin and galbanic acid combination therapy with some common chemotherapeutics in colon carcinoma cells. *Avicenna J. Phytomed.,* **2019**, *9*(3), 237-247. PMID: 31143691

[31] Kim, Y.H.; Shin, E.A.; Jung, J.H.; Park, J.E.; Koo, J.; Koo, J.I.; Shim, B.S.; Kim, S.H. Galbanic acid potentiates TRAIL induced apoptosis in resistant non-small cell lung cancer cells *via* inhibition of MDR1 and activation of caspases and DR5. *Eur. J. Pharmacol.,* **2019**, *847*, 91-96.

http://dx.doi.org/10.1016/j.ejphar.2019.01.028 PMID: 30689998

[32] Zhang, Y.; Kim, K.H.; Zhang, W.; Guo, Y.; Kim, S.H.; Lü, J. Galbanic acid decreases androgen receptor abundance and signaling and induces G1 arrest in prostate cancer cells. *Int. J. Cancer,* **2012**, *130*(1), 200-212.
http://dx.doi.org/10.1002/ijc.25993 PMID: 21328348

[33] Oh, B.S.; Shin, E.A.; Jung, J.H.; Jung, D.B.; Kim, B.; Shim, B.S.; Yazdi, M.C.; Iranshahi, M.; Kim, S.H. Apoptotic effect of galbanic acid *via* activation of caspases and inhibition of Mcl-1 in H460 non-small lung carcinoma cells. *Phytother. Res.,* **2015**, *29*(6), 844-849.
http://dx.doi.org/10.1002/ptr.5320 PMID: 25753585

[34] Kazemi, M.; Kouhpeikar, H.; Delbari, Z.; Khodadadi, F.; Gerayli, S.; Iranshahi, M.; Mosavat, A.; Behnam Rassouli, F.; Rafatpanah, H. Combination of auraptene and arsenic trioxide induces apoptosis and cellular accumulation in the subG1 phase in adult T-cell leukemia cells. *Iran. J. Basic Med. Sci.,* **2021**, *24*(12), 1643-1649.
PMID: 35432798

[35] Delbari, Z. Combination of umbelliprenin and arsenic trioxide acts as an effective modality against T-cell leukemia/lymphoma cells. *Nat. Prod. Commun.,* **2022**, *17*(1), 1934578X211072334.

[36] Kouhpaikar, H.; Sadeghian, M.H.; Rafatpanah, H.; Kazemi, M.; Iranshahi, M.; Delbari, Z.; Khodadadi, F.; Ayatollahi, H.; Rassouli, F.B. Synergy between parthenolide and arsenic trioxide in adult T-cell leukemia/lymphoma cells *in vitro. Iran. J. Basic Med. Sci.,* **2020**, *23*(5), 616-622.
PMID: 32742599

[37] Lau, A.; Nightingale, S.; Taylor, G.P.; Gant, T.W.; Cann, A.J. Enhanced MDR1 gene expression in human T-cell leukemia virus-I-infected patients offers new prospects for therapy. *Blood,* **1998**, *91*(7), 2467-2474.
http://dx.doi.org/10.1182/blood.V91.7.2467 PMID: 9516147

[38] Ariumi, Y.; Kaida, A.; Lin, J.Y.; Hirota, M.; Masui, O.; Yamaoka, S.; Taya, Y.; Shimotohno, K. HTLV-1 tax oncoprotein represses the p53-mediated trans-activation function through coactivator CBP sequestration. *Oncogene,* **2000**, *19*(12), 1491-1499.
http://dx.doi.org/10.1038/sj.onc.1203450 PMID: 10734308

[39] Haller, K.; Ruckes, T.; Schmitt, I.; Saul, D.; Derow, E.; Grassmann, R. Tax-dependent stimulation of G1 phase-specific cyclin-dependent kinases and increased expression of signal transduction genes characterize HTLV type 1-transformed T cells. *AIDS Res. Hum. Retroviruses,* **2000**, *16*(16), 1683-1688.
http://dx.doi.org/10.1089/08892220050193146 PMID: 11080810

[40] Mori, N.; Fujii, M.; Ikeda, S.; Yamada, Y.; Tomonaga, M.; Ballard, D.W.; Yamamoto, N. Constitutive activation of NF-kappaB in primary adult T-cell leukemia cells. *Blood,* **1999**, *93*(7), 2360-2368.
PMID: 10090947

[41] Sun, S.C.; Yamaoka, S. Activation of NF-kappaB by HTLV-I and implications for cell transformation. *Oncogene,* **2005**, *24*(39), 5952-5964.
http://dx.doi.org/10.1038/sj.onc.1208969 PMID: 16155602

[42] Yoshida, M. Multiple viral strategies of HTLV-1 for dysregulation of cell growth control. *Annu. Rev. Immunol.,* **2001**, *19*(1), 475-496.
http://dx.doi.org/10.1146/annurev.immunol.19.1.475 PMID: 11244044

[43] Kashanchi, F.; Brady, J.N. Transcriptional and post-transcriptional gene regulation of HTLV-1. *Oncogene,* **2005**, *24*(39), 5938-5951.
http://dx.doi.org/10.1038/sj.onc.1208973 PMID: 16155601

[44] Matsuoka, M.; Jeang, K-T. Human T-cell leukaemia virus type 1 (HTLV-1) infectivity and cellular transformation. *Nat. Rev. Cancer,* **2007**, *7*(4), 270-280.
http://dx.doi.org/10.1038/nrc2111 PMID: 17384582

[45] Sherr, C.J.; Roberts, J.M. Inhibitors of mammalian G1 cyclin-dependent kinases. *Genes Dev.,* **1995**, *9*(10), 1149-1163.
http://dx.doi.org/10.1101/gad.9.10.1149 PMID: 7758941

[46] Djerbi, M.; Screpanti, V.; Catrina, A.I.; Bogen, B.; Biberfeld, P.; Grandien, A. The inhibitor of death receptor signaling, FLICE-inhibitory protein defines a new class of tumor progression factors. *J. Exp. Med.,* **1999**, *190*(7), 1025-1032.
http://dx.doi.org/10.1084/jem.190.7.1025 PMID: 10510092

[47] Medema, J.P.; de Jong, J.; van Hall, T.; Melief, C.J.; Offringa, R. Immune escape of tumors *in vivo* by expression of cellular FLICE-inhibitory protein. *J. Exp. Med.,* **1999**, *190*(7), 1033-1038.
http://dx.doi.org/10.1084/jem.190.7.1033 PMID: 10510093

[48] Okamoto, K.; Fujisawa, J.; Reth, M.; Yonehara, S. Human T-cell leukemia virus type-I oncoprotein Tax inhibits Fas-mediated apoptosis by inducing cellular FLIP through activation of NF-kappaB. *Genes Cells,* **2006**, *11*(2), 177-191.
http://dx.doi.org/10.1111/j.1365-2443.2006.00927.x PMID: 16436054

[49] Ozaki, T.; Nakagawara, A. p53: The attractive tumor suppressor in the cancer research field. *J. Biomed. Biotechnol.,* **2011**, *2011*, 603925.
http://dx.doi.org/10.1155/2011/603925 PMID: 21188172

[50] Xu-Monette, Z.Y.; Medeiros, L.J.; Li, Y.; Orlowski, R.Z.; Andreeff, M.; Bueso-Ramos, C.E.; Greiner, T.C.; McDonnell, T.J.; Young, K.H. Dysfunction of the TP53 tumor suppressor gene in lymphoid malignancies. *Blood,* **2012**, *119*(16), 3668-3683.
http://dx.doi.org/10.1182/blood-2011-11-366062 PMID: 22275381

[51] Bartke, T.; Siegmund, D.; Peters, N.; Reichwein, M.; Henkler, F.; Scheurich, P.; Wajant, H. p53 upregulates cFLIP, inhibits transcription of NF-kappaB-regulated genes and induces caspase-8-independent cell death in DLD-1 cells. *Oncogene,* **2001**, *20*(5), 571-580.
http://dx.doi.org/10.1038/sj.onc.1204124 PMID: 11313989